Proceedings of the DIS'2004, Štrbské Pleso, Slovakia

MEASUREMENT OF THE ELECTROMAGNETIC COMPONENT OF PHOTON LIGHT-CONE WAVE FUNCTION AT HERA

JUSTYNA MAGDALENA UKLEJA
Warsaw University
Hoża 69, Warsaw, Poland
E-mail: jtomasz@fuw.edu.pl

This paper reports the measurement of the electromagnetic component of the photon light-cone wave function. This component was measured with the ZEUS detector at HERA in the exclusive production of dimuons, $ep \to e\mu^+\mu^- p$.

1 Introduction

The internal structure of hadrons and the photon may be described using light cone wave functions (LCWF), which are essential for understanding their interactions. The photon LCWF has both electromagnetic and hadronic components:

$$\begin{aligned}\psi_\gamma = {} & a|\gamma_p\rangle + b|l^+l^-\rangle + c|l^+l^-\gamma\rangle + (other\ e.m.) \\ & +d|q\bar{q}\rangle + e|q\bar{q}g\rangle + (other\ hadronic) + \dots\ , \end{aligned} \tag{1}$$

where $|\gamma_p\rangle$ describes the point bare photon and $|l^+l^-\rangle$ stands for $|e^+e^-\rangle$, $|\mu^+\mu^-\rangle$ etc. Each of these states is a sum over the relevant helicity components. The wave function of the photon is very rich: it can be studied for real photons, for virtual photons of different virtualities, for transverse and for longitudinal photons. The electromagnetic component of the photon LCWF can be calculated within QED while the hadronic component is model dependent.

The measurements presented here are based on the method applied for the pion LCWF in diffractive dissociation [1, 2]. This method was shown to be sensitive to the structure of the LCWF.

2 Data analysis

In this paper a measurement of the electromagnetic component of the real photon LCWF is presented based on the exclusive $ep \to e\mu^+\mu^- p$ photoproduction process. The analysis used data collected with the ZEUS detector during 1999-2000 [3], which corresponds to an integrated luminosity of $55.4\,\mathrm{pb}^{-1}$. During that time HERA collided 920 GeV protons and 27.5 GeV positrons. Events were selected by requiring two oppositely-charged tracks in the central tracking detector (CTD)

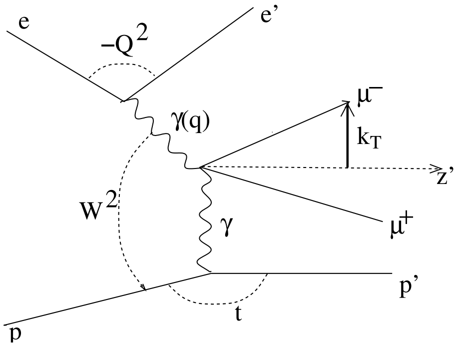

$$
\begin{aligned}
u &= \frac{E_1 + p_{z1}}{E_1 + p_{z1} + E_2 + p_{z2}} \\
W^2 &= (q+P)^2 \sim 2E_p \sum_i (E_i + p_{zi}) \\
t &= (P - P')^2 \sim p_T^2(\mu\mu) \\
M^2_{\mu\mu} &= (p_1 + p_2)^2 \\
\vec{k}_{T1} + \vec{k}_{T2} &= \vec{0}
\end{aligned}
$$

Figure 1. Definition of the kinematic variables.

which were associated to the primary vertex and matched with energy deposits in the calorimeter (no signal from the scattered positron was required). An additional requirement that no other activity in the calorimeter was observed was made and the energy measured in the forward plug calorimeter (placed downstream close to the beam) had to be less than 1 GeV to reduce the contribution from proton dissociation. The kinematic variables, defined in Fig.1, were reconstructed from the momenta of the CTD tracks: u is the longitudinal momentum fraction carried by the positively-charged muon; W is the γp centre of mass energy; t is the square of the four momentum transfer at the proton vertex; $M_{\mu\mu}$ is the invariant mass of the dimuon system and k_T is the transverse momentum of one of the muons with respect to the photon. E_1, p_1 and E_2, p_2 are energies and momenta of the positive and negative muon, respectively.

The analysis was performed in the following kinematic region: $4 < M_{\mu\mu} < 15\,\mathrm{GeV}$, $30 < W < 170\,\mathrm{GeV}$, $|t| < 0.5\,\mathrm{GeV}^2$, $0.1 < u < 0.9$ and $k_T > 1.2\,\mathrm{GeV}$. The contribution from proton dissociative events was determined to be 11.0±1.0% and was substracted from the data. The acceptance corrections and resolution effects were determined using the generator Monte Carlo GRAPE [4] for dilepton production in ep collisions, interfaced to PYTHIA [5].

3 Results

The measured k_T, W, t and $M_{\mu\mu}$ distributions are presented in Fig. 2. The data are compared with the GRAPE prediction which takes into account both elastic and proton dissociative events. Good agreement is seen between data and MC in shape and normalisation.

The cross section as a function of u is presented in Fig. 3 and compare to theory (BFGMS) [6] which has been normalised to the data. The data were also compared

to the predictions from GRAPE [7]. Both predictions describe the data reasonably well.
The measurements presented here provide the evidence that quasi-elastic processes can be reliably used to measure LCWFs.

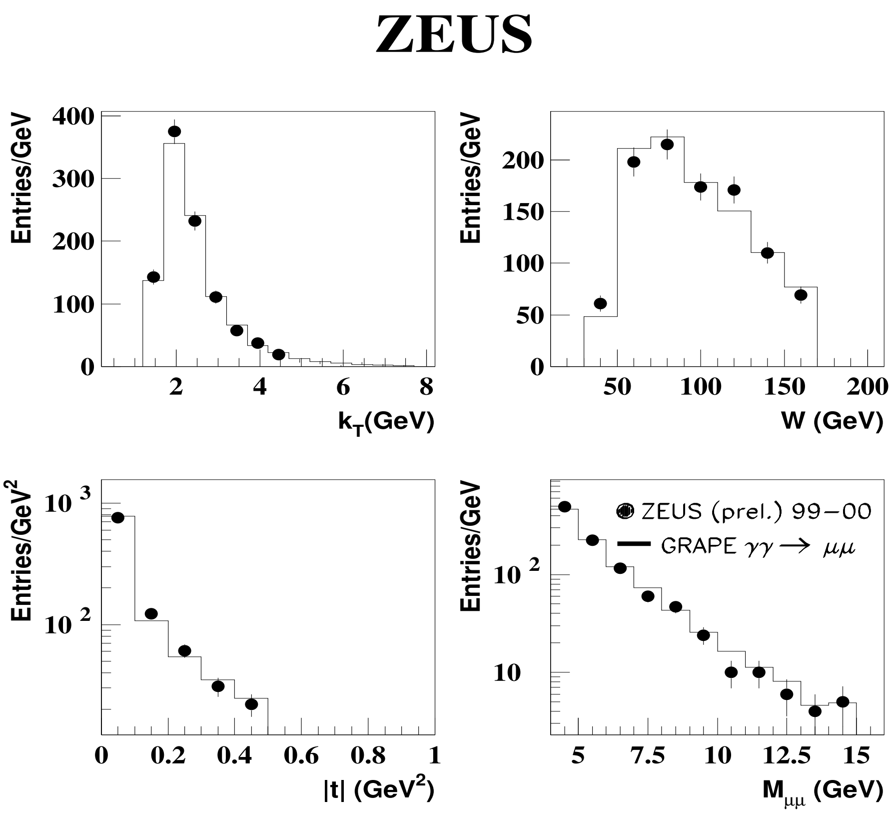

Figure 2. Comparison of the detector-level distributions observed in data and MC, prior is the subtraction of the proton dissociation contribution. The error bar show the statistical uncertainties.

References

1. E791 Coll., E.M.Aitala et al., Phys. Rev. Lett. **86**, 4768 (2001).
2. E791 Coll., E.M.Aitala et al., Phys. Rev. Lett. **86**, 4773 (2001).
3. ZEUS Coll. (ed.), *The ZEUS Detector*. Status Report (unpublished), DESY (1993), available on `http://www-zeus.desy.de/bluebook/bluebook.html`.

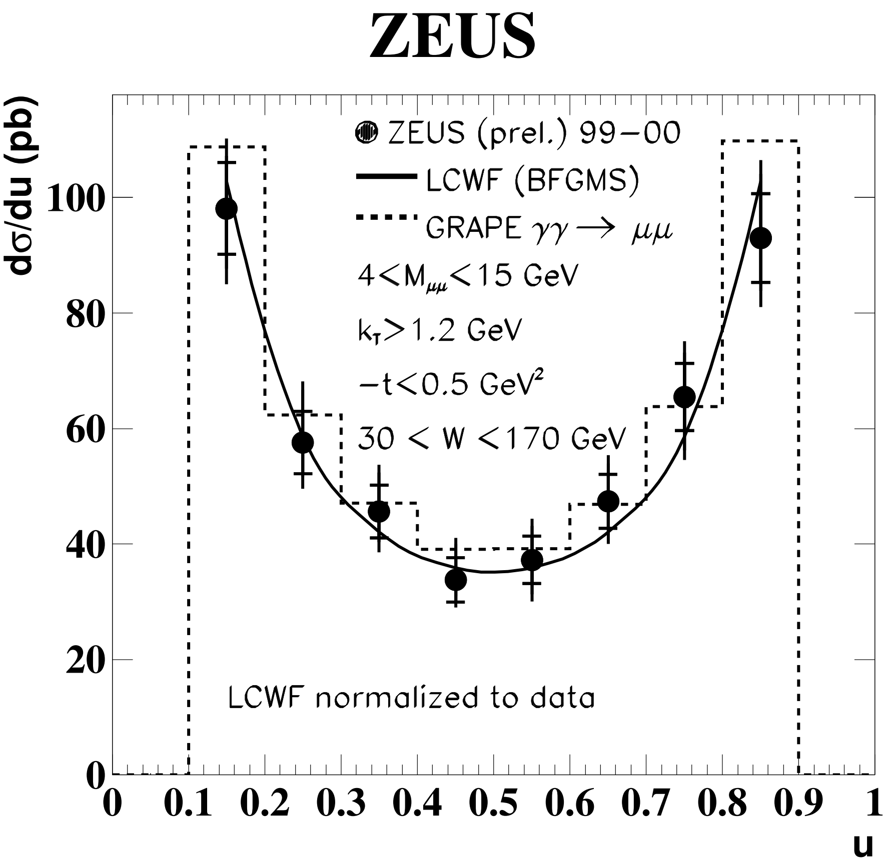

Figure 3. The differential cross section $d\sigma/du$ measured for $30 < W < 170\,\mathrm{GeV}$, $4 < M_{\mu\mu} < 15\,\mathrm{GeV}$, $k_T > 1.2$ GeV and $|t| < 0.5$ GeV^2. The dashed histogram showns the predictions from GRAPE Monte Carlo. The solid curve represents the BFGMS prediction for the photon LCWF [6]. The inner error bars show the statistical uncertainties, while the outer errors bars show the statistical and systematic uncertainties added in quadrature.

4. T. Abe et al., *Proc. Workshop on Monte Carlo Generators for HERA Physics*, T.A. Doyle et al. (ed.), p. 566. DESY, Hamburg, Germany (1999). Also in preprint DESY-PROC-1999-02, available on `http://www.desy.de/~heramc/`.
5. H.-U. Bengtsoon and T. Sjöstrand, Comp. Phys. Comm. **46**, 43 (1987).
6. S. J. Brodsky, L. Frankfurt, J. F. Gunion, A. H. Mueller and M. Strikman, Phys. Rev. **D50**, 3134 (1994).
7. T. Abe, Comp. Phys. Comm. **136**, 126 (2001).